

Comparative assessment of landslide susceptibility by logistic regression and first order second moment method: Case study of Bujumbura Peri-Urban Area, Burundi.

Gervais Shirambere*, Maurice Nyadawa**, Jean pierre Masekanya***, Timothy Nyomboi****

*(*Institute for Basic Sciences Technology and Innovation, Pan African University, Juja, Kenya*)

** (*Jaramogi Oginga Odinga University of Science and Technology, Bondo, Kenya*)

***(*Université du Burundi, Bujumbura, Burundi*)

****(*Moi University, Eldoret, Kenya*)

Corresponding Author : Gervais Shirambere

ABSTRACT

Several landslides incidents in the Bujumbura region are reported regularly by independent sources. However, few studies on the causes in the region have been conducted and no record of susceptibility map at a regional exists. In this study, two different approaches are applied to map landslide susceptibility in the region. The physical approach is based on mohr-coulomb failure criterion and is applied using a probabilistic approach, the first order second moment method. The statistical approach is based on logistic regression. The study has two objectives: (i) to map landslide susceptibility in the region and (ii) to compare the results of the different approaches. Applying the two approaches in a GIS framework, two susceptibility map are produced. The accuracy of the two models is independently assessed using ROC and AUC curves. A comparative analysis of the results is conducted and the results shows a fair spatial correlation. The susceptibility maps are compared using rank differences and ArcSDM and a spatial comparison map of susceptibility levels is produced.

Keywords – Shallow landslide, FOSM, Logistic regression, Bujumbura

Date of Submission: 09-08-2018

Date of acceptance: 24-08-2018

I. INTRODUCTION

The peri-urban area of Bujumbura, hereafter referred to as Bujumbura region, has witnessed several hazards of different nature: floods, mudflows and landslides. The impact of landslides includes loss of life, destruction of infrastructure, damage to land and loss of natural resources [1], [2]. Motivated by the increasing number of recorded incidents, Nibigira et al. (2015) mapped past and existing landslides in the western part of Burundi, which includes the Bujumbura region, and identified factors influencing the development of instabilities [3]. In order to provide information about landslide susceptibility for one watershed of the Bujumbura region, Kubwimana et al. (2018) developed a landslide susceptibility map using Analytic Hierarchy Process (AHP) for the Kanyosha river watershed [4]. The objectives of this study is to develop landslide susceptibility maps from logistic regression and deterministic model, and to asses and compare the accuracy of the obtained susceptibility maps.

Several studies assessing and mapping landslide susceptibility have been conducted worldwide using two principal approaches: physical and statistical. On one hand, physically based

approaches [5]–[9] have been extensively applied for landslide susceptibility assessment. For physically based models, the relevant factor is the factor of safety based on slope stability analysis. Slope stability analyses of landslides in physically based models are usually performed using conventional limit equilibrium method based on the Mohr–Coulomb failure criterion. On the other hand, statistical approaches [10]–[14] have been also used for landslide susceptibility assessment. Statistical approaches are more bounded to local particularities since they are always linked to a determined training dataset. Few comparative assessments of the two approaches have been conducted [15], [16]. Recent studies have developed a new physically based slope stability analysis for unsaturated soils [17].

This study proposes a comparative assessment of the new physical approach and a statistical approach, the logistic regression. For comparative purposes the physical approach is developed using a probabilistic method, the first order second moment method.

In this study, one physical approach based on Lu and Godt (2008) definition of the safety factor and one statistical approach based on logistic

regression, both within a geographical information system(GIS), were applied to map and assess landslide susceptibility in the Bujumbura region. For the first purpose of mapping landslide susceptibility, two set of independent variables were collected: independent variables of the physical model and independent variables for the statistical model. Independent variables of the physical model were based on the Lu and Godt [17] model of slope stability. For the statistical model, a number of five predictors using expert knowledge were established as the independent variables of the logistic regression. Using GIS the two models were applied and landslide susceptibility was mapped. Finally, accuracy of the two model was assessed using the success rate curve and compared using kappa statistics and rank differences.

II. STUDY AREA

The area under study is located in western part of Burundi near the Tanganyika Lake, lying between 3°28'S and 3°23'S latitude, and 29°20'E and 29°24'E longitude (**Error! Reference source not found.** and Figure 1). The area is around 31 km² and includes 15 administrative sectors. The study area overlaps two geographical region of Burundi: Imbo Region and Mirwa Region. The Imbo region is a relatively flat region and the



Figure 1. Location of study area

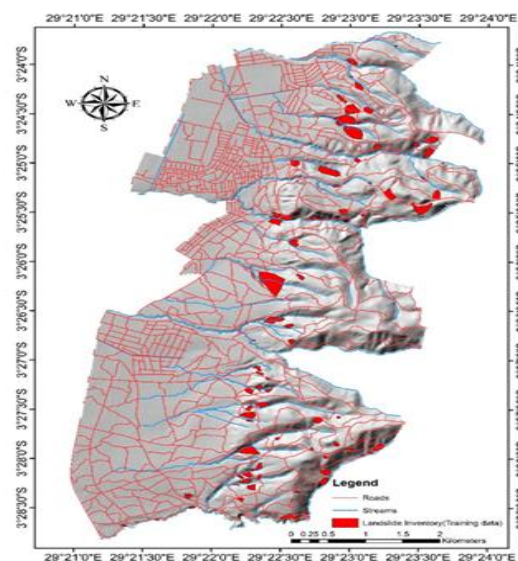


Figure 1. Extent of the study map

Mirwa region is composed of steep hills and mountains. The study area also overlaps watersheds of three of the major rivers across Bujumbura. The altitude varies from 777 to 1386 m. The slope angle values range from 0° to 57°. The yearly average temperature is 23 °C, and the annual precipitation is 1274 mm [18].

III. DATA AND METHODOLOGY

3.1. Landslide Inventory

Within the framework of this study a landslide inventory map was required both for application in the logistic regression model and for accuracy assessment of both landslide models. For this purpose, a landslide inventory was prepared using literature review, aerial orthophotos, satellite imagery (Google earth Imagery), a 10 m-resolution Digital Elevation Model (DEM) provided by the “Bureau de centralisation géomatique du Burundi” (BCG) and extensive field survey. In result, a detailed and reliable inventory map with a total of 89 landslides was created (Figure 1).

The identified landslides were classified mainly as shallow translational slides according to classification proposed by Varnes [19]. Since the aim of this study is assessing the accuracy of models, only one training dataset was established. The training dataset was then used in inferring the weights of selected predisposing factors. Finally, the training dataset was used for accuracy assessment for both models and for their comparison using success rate curves.

3.2. Statistical model

For statistical models, logistic regression is widely used in landslide susceptibility assessment and mapping [10], [12], [14], [20] – [24]. In this study a binary logistic regression was applied.

Logistic regression is a statistical method involving multivariate regression in order to link a dependent variate with multiple independent variables. The binary logistic regression used in this study is used to predict presence or absence of landslide based on the weights of independent variables. Among numerous benefits of using logistic regression, there is the possibility to use different independent variables (categorical or continuous) and the fact that no assumptions about the distribution of independent variables is made a priori. The logistic regression defines a probability of landslide using relationship given by:

$$P = e^y / (1 + e^y) \quad (1)$$

where P is the probability of landslide occurrence and y is the linear logistic model. The values of the linear logistic model theoretically vary from $-\infty$ to $+\infty$. Hence the probability defined by (1) ranges between 0 and 1. The linear logistic model is defined by the relationship:

$$y = b_0 + b_1x_1 + \dots + b_nx_n \quad (2)$$

where b_0 is the intercept of the model, b_1, \dots, b_n are the coefficients of the independent variables, x_1, \dots, x_n are the independent variables. Amid various predisposing factors, five important predictors were selected: Pedology, Land Cover, Slope Angle, Distance to streams and Distance to roads. The selected predisposing factors are already successfully applied in other research on this topic [25]. Two independent variables (Pedology and Land cover) are categorical and the rest of the independent variables are continuous variables (Slope angle, Distance to streams and Distance to roads). Pedology is a major factor in soil stability. The depth of a shallow landslide is generally not more than 1–2 m. Therefore, the pedological map provides a useful basis for the study of the relationship between landslides and the type of soils [26]. The map used in this study was derived from the 1:50.000 soil map of Burundi provided by the “Institut Geographique du Burundi” (IGEBU). The map is composed of five types of soils (Figure 2)

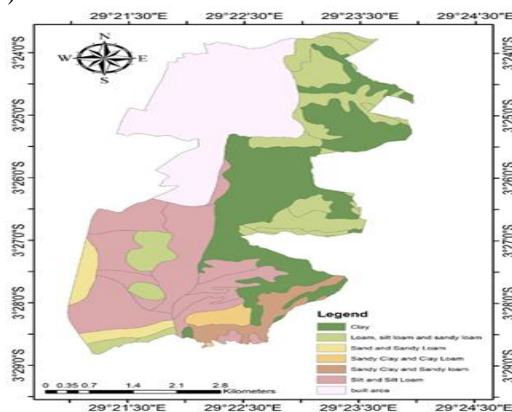


Figure 2. Pedology Map

Land cover variations highly influence landslide formation and evolution. Statistical analysis through logistic regression has proved to be a convenient tool for assessing the influence of different land cover classes on landslides. Several classes have been found to significantly increase or decrease the rate of landslides [27]. The map used in our study was clipped from Sentinel-2 global land cover data by the Regional Center for Mapping of Resources of Development (RCMRD) (Figure 3).

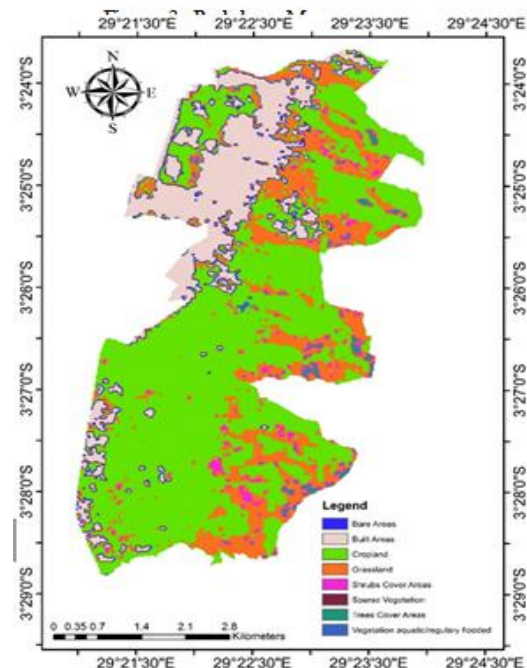


Figure 3. Land Cover Map

Slope angle, distance to streams and distance to roads are all important factors in landslide assessment. Most of the studies selected either one or all those factors in modeling landslide susceptibility [3], [24], [28], [29]. In this study a 10 m-resolution Digital Elevation Model (DEM) in combination with roads and streams maps provided by the IGEBU were used for distance and angle computing using ArcGIS 10.3 (Figure 1). First Order Second Moment Method A number of deterministic model have been applied in various context [6], [7], [9]. Lu and Godt (2008) introduced a generalized framework for the stability of infinite slopes under steady unsaturated seepage conditions. As all the deterministic models, the purpose is to determine a safety factor reflecting the stability of a considered slope. The proposed framework by Lu and Godt relies on the existing understanding of unsaturated-

zone hydrology and considers for the first time, the contribution of suction stress in the stress analysis. The safety factor is defined by the relationship:

$$FS = \frac{\tan\phi'}{\tan\beta} + \frac{2c'}{\gamma H \sin 2\beta} - \frac{\sigma^s}{\gamma H} (\tan\beta + \cot\beta) \tan\phi' \quad (3)$$

where ϕ' is the friction angle; β is the slope angle; c' is the soil cohesion; γ is the unit weight of moist soil; H is the height of the soil column above the bedrock and σ^s is the suction stress defined by:

$$\sigma^s = \begin{cases} \frac{1}{\alpha} \ln[(1 + q/k_s)e^{-\gamma_w \alpha z} - q/k_s] & u_a - u_w \leq 0 \\ \frac{1}{\alpha} \frac{\ln[(1 + q/k_s)e^{-\gamma_w \alpha z} - q/k_s]}{[1 + (-\ln[(1 + q/k_s)e^{-\gamma_w \alpha z} - q/k_s])^n]^{(n-1)/n}} & u_a - u_w > 0 \end{cases} \quad (4)$$

where k_s is the field hydraulic conductivity; q is the steady infiltration; γ_w is the unit weight of water; α and n are the empirical fitting parameters of unsaturated soils properties and the matric suction $u_a - u_w$ is defined by:

$$u_a - u_w = -\frac{1}{\alpha} \ln[(1 + q/k_s)e^{-\gamma_w \alpha z} - q/k_s] \quad (5)$$

The need of a probabilistic approach is essential to this work since it will help compare the statistical and the deterministic model. There are several methods such as the point estimate method [30], first order second moment [31], [32] or Monte Carlo simulation [33] which are usually combined with a slope stability model to provide a probability of landslide instead of a safety factor. In this work the first order second moment method (FOSM) was used combined with Lu and Godt safety factor equation to map landslide susceptibility. The FOSM uses the first-order terms of a Taylor series

approximation of the performance function to estimate the expected value and variance of the performance function. Since FOSM's highest statistical value is variance, the method is called a second moment method. The usual Taylor's series approximation is:

$$Z = g(\mu_{\bar{x}}) + \sum_{i=1}^n \frac{\partial g(\mu_{\bar{x}})}{\partial x_i} (x_i - \mu_{x_i}) + \frac{1}{2} \sum_{i=1}^n \sum_{j=1}^n \frac{\partial^2 g(\mu_{\bar{x}})}{\partial x_i \partial x_j} (x_i - \mu_{x_i}) (x_j - \mu_{x_j}) + \dots \quad (6)$$

where Z is the performance function which is in our case the FS and the mean value of $FS = g(\mu_{\bar{x}})$; $\mu_{\bar{x}}$ is the mean value vector of $(x_1, x_2, x_3, \dots, x_n)$ and μ_{x_i} is the mean value of each x_i ,

Considering as proposed in this method only the order term, the mean value of the safety factor and the variance of the safety factor become:

$$\overline{FS} = g(\mu_{\bar{x}}) = g(\mu_{x_1}, \mu_{x_2}, \dots, \mu_{x_n}) = FS(\bar{x}) \quad (7)$$

$$\text{var}(Z) = \sigma_{FS}^2 = \sum_{i=1}^n \sum_{j=1}^n \frac{\partial g(\mu_{\bar{x}})}{\partial x_i} \frac{\partial g(\mu_{\bar{x}})}{\partial x_j} \text{cov}(x_i, x_j) \quad (8)$$

where $\text{cov}(x_i, x_j)$ is the covariance of x_i and x_j . However, our variables are considered uncorrelated. Hence, the variance of the safety factor becomes:

$$\text{var}(Z) = \sigma_{FS}^2 = \sum_{i=1}^n \left(\frac{\partial g(\mu_{\bar{x}})}{\partial x_i} \right)^2 s_{x_i}^2 \quad (9)$$

$$\text{var}(Z) = \left[\frac{1 + \tan^2 \phi}{\tan \beta} + \frac{(1 + \tan^2 \phi) + (\tan \beta + \cot \beta) + \sigma^s}{\gamma H} \right]^2 * s_{\phi}^2 + \left(\frac{2}{\gamma H \sin 2\beta} \right)^2 * s_c^2 + \left[\frac{-2c}{\gamma^2 H \sin 2\beta} + \frac{-\sigma^s (\tan \beta + \cot \beta) \tan \phi}{\gamma^2 H} \right]^2 * s_{\sigma^s}^2 \quad (10)$$

Table 1. Mean and standard deviation of mechanical and Hydrological parameters

Sector	Friction Angle, degrees		Cohesion, kPa		Hydraulic Conductivity, mm/s		α	n	Soil Density, kN/m ³	Bulk
	Mean	St.Dev	Mean	St.Dev	Mean	St.Dev				
Ngongo	34.860	1.040	22.680	4.461	0.076	0.000	0.044	1.156	14.351	0.103
Sagamba	35.447	1.851	27.453	11.845	0.083	0.032	0.066	1.162	13.834	0.595
Kinama	34.867	2.307	19.507	9.187	0.117	0.055	0.063	1.224	12.714	0.234
Benge	37.680	3.301	31.600	10.315	0.056	0.000	0.038	1.168	14.478	0.237
Gihinga	35.453	1.524	40.887	10.139	0.058	0.000	0.041	1.170	14.270	0.287
Ruyange	34.840	2.573	29.460	13.312	0.102	0.045	0.059	1.187	13.051	0.294
Nyamutenderi	39.020	1.236	14.000	4.879	0.048	0.000	0.063	1.168	12.946	0.268
Kibuye	26.180	6.257	38.140	6.465	0.092	0.000	0.052	1.184	13.271	0.272
Rweza	25.280	1.849	36.680	17.513	0.110	0.032	0.046	1.153	14.258	0.218
Kizingwe-Bihara	31.453	5.861	39.720	21.587	0.089	0.000	0.047	1.199	13.604	0.353
Kanyosha	38.200	4.975	26.120	19.162	0.069	0.000	0.045	1.162	14.140	0.231
Kamesa	35.100	1.666	22.600	12.665	0.069	0.000	0.063	1.183	12.946	0.225
Kinanira I	37.200	5.703	17.260	10.789	0.059	0.000	0.033	1.166	15.050	0.229
Gitarumuka	30.540	6.390	48.320	22.543	0.093	0.000	0.060	1.237	12.770	0.320
Gasekebuye	33.640	3.568	44.380	12.806	0.076	0.000	0.044	1.162	14.511	0.093

In order to apply a deterministic model, an extensive laboratory and field survey was conducted. A statistically meaningful sample of 225 (15 for each sector) samples were collected for laboratory analysis and the same number of field test were performed. At each sector level, a mean average value and a standard deviation for the concerned parameters were inferred from laboratory analysis (Table 1).

Friction angle and cohesion are key parameters to landslide formation. The lower the cohesion intercept, the higher the probability of landslide occurrence. The lower the friction angle, the lower the probability of landslide occurrence. However, these parameters are highly variable spatially. Hence in our approach we randomly selected sample point to measure specifically the mean and the spread at the sector level for all these parameters. The combination of the mechanical parameters with other local parameters such as slope angle and depth at each location will provide an accurate mean value of the safety factor since the variation of these parameters is taken in account in our probabilistic approach. Friction angle and cohesion were determined using laboratory procedures [34].

The definition of the depth of soils is difficult to conduct on a regional scale. In this study a soil depth model, using a simplified approach often used in largescale regional analyses, is applied [35]. The considered model correlates soil depth to the local slope and has the form:

$$H_i = H_{max} \left[1 - \frac{\tan \beta_i - \tan \beta_{min}}{\tan \beta_{max} - \tan \beta_{min}} \left(1 - \frac{H_{min}}{H_{max}} \right) \right] \quad (11)$$

where H_i is the computed soil depth, H_{max} and H_{min} are respectively, the maximum and the minimum soil depth measured in the area, β_i is the local slope angle value and β_{max} and β_{min} are respectively maximum and minimum slope angle value measured in the area.

The hydraulic conductivity of soils was determined by the simple falling head technique [36]. This method has been developed and applied on Burundian soils. The Simplified Falling Head (SFH) technique allows us to determine the field-saturated hydraulic conductivity of an initially unsaturated soil by a one-dimensional falling head infiltration process. The SFH technique consists of applying quickly a small volume of water on the soil surface confined by a ring inserted at a fixed distance into the soil, H_0 , and in measuring the time, t_a , from the application of water to the instant at which the infiltration surface is no longer covered by water. The hydraulic conductivity takes the form:

$$K_{fs} = \frac{\Delta\theta}{(1-\Delta\theta)t_a} \left[\frac{H_0}{\Delta\theta} - \frac{(H_0 + \frac{1}{\alpha^*})}{1-\Delta\theta} \ln \left(1 + \frac{(1-\Delta\theta)H_0}{\Delta\theta(H_0 + \frac{1}{\alpha^*})} \right) \right] \quad (12)$$

where $\Delta\theta$ is the difference between the field-saturated (θ_{fs}) and the initial (θ_i) volumetric soil water content and α^* is parameter based on the textural/structural soil characteristics.

Van Genuchten parameters are used to determine suction stress for unsaturated soils. In our study, a pedo-transfer function was applied estimates the water retention curve characteristics using only soil texture and bulk density [37]. For this purpose, applied standard laboratory procedures to obtain particle size distribution and bulk density [38], [39].

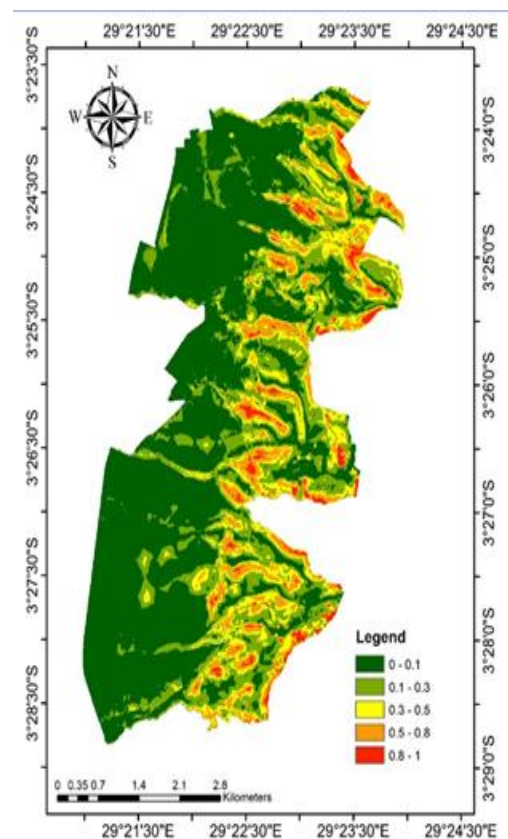


Figure 4. Landslide susceptibility map. (LR)

3.3. Model comparison.

For model comparison we first classified the obtained maps according to the same levels of susceptibility (>0.8 =very high, $0.5-0.8$ =high, $0.3-0.5$ =moderate, $0.3-0.1$ =low, <0.1 =very low) and defined the effective ratios for each level. Then using the Rank Differences tool of the ArcSDM package [40] we assessed the models concordance. Further, we used kappa statistics to assess spatial correlation. Finally, we used ROC (receiver operating characteristic) curves and AUC (Area

Under the receiver operating characteristic Curve) to assess independently the accuracy of each model compared to the training dataset.

IV. RESULTS AND DISCUSSION

4.1. Statistical landslide susceptibility assessment

Landslide susceptibility map obtained using logistic regression (Fig. 5) shows that 10.4% of the study area is under very high and high probability of landslide. The accuracy of the logistic regression model applied is 85.537%. The logistic regression model applied correctly identified 38.268% of landslide in the training dataset and correctly identified 95.372% of the training dataset not affected by landslide. The precision of the logistic regression model applied is 63.243% (Table 2).

Table 2. Confusion matrix of the Logistic Regression Model

Observed		Predicted		Percentage Correct
		landslide	no landslide	
landslide	no landslide	34149	1657	95.372
	landslide	4599	2851	38.268
	Overall Percentage			85.537

The coefficients of the logistic regression model applied (beta weights) for each predisposing factor are listed in Table 3. For the continuous variables, the odds of landslides increase when the slope angle and the distance to roads increases and vice versa when the distance to streams increases, the odds of landslides decreases. For the categorical variables, the odds of landslides are higher for predominantly sandy soils and lower for predominantly clayey and loamy soils. Likewise, the odds of landslides for shrubs covered and trees covered area are higher than the rest of land cover type. However, this is mainly due to the soil occupation density of the study area where shrubs and trees covered areas are located only in the steepest slopes and built or cropland areas on more gentle slopes.

The ROC curve of the landslide susceptibility model is shown in Fig. 7. The LR model predictive capacity is good, as expressed by the AUC of 0.872.

4.2. Physically based landslide susceptibility assessment

Landslide susceptibility map produced using the FOSM shows that 5.4% of the study area is under very high and high probability of landslide (Fig. 6). The accuracy of the FOSM model applied is 82.446%. The FOSM model applied correctly identified 13.96% of landslide in the training dataset and correctly identified 96.696% of the training

Table 2. Description of landslides factors and unstandardized weights

Factor	ID	Description	N _e of pixels	Frequency %	N _e of pixels with Landslide	Beta weights	Odds ratio
Pedology	P0	Built area	76744	25.2	699	-0.248	0.780
	P1	Sand and Sandy Loam	9063	3	63	1.938	6.943
	P2	Sandy Clay and Clay Loam	4823	1.6	399	0	1
	P3	Clay	78201	25.6	3111	-0.246	0.782
	P4	Sandy Clay, Sandy clay loam and Sandy loam	10829	3.6	412	0.419	1.521
	P6	Silt and Silt Loam	73533	24.1	1002	-0.458	0.632
	P7	Loam. silt loam and sandy loam	51685	17	1764	-0.328	0.720
Land cover	L1	Trees Cover Areas	3115	1	76	2.095	8.127
	L2	Shrubs Cover Areas	7549	2.5	418	0	1
	L3	Grassland	53678	17.6	2588	-0.722	0.486
	L4	Cropland	175727	57.6	3728	-1.241	0.289
	L5	Vegetation aquatic/regularly flooded	6577	2.2	284	-0.572	0.564
	L6	Sparse Vegetation	6764	2.2	136	-1.214	0.297
	L7	Bare Areas	4364	1.4	83	-1.509	0.221
	L8	Built Areas	47104	15.5	137	-2.763	0.063
Slope angle					0.070	1.072	
Distance to streams					-0.009	0.991	
Distance to roads					0.014	1.014	

dataset not affected by landslide. The precision of the logistic regression model applied is 46.783% (Table 4). The landslide susceptibility map produced spatially approximates the slope angle map. This is due to the contribution of the slope angle variable in each of the component of the safety factor equation.

Table 4. Confusion matrix of the FOSM model

Observed		Predicted		Percentage Correct
		no landslide	landslide	
landslide	no landslide	34623	1183	96.696
	landslide	6410	1040	13.960
Overall Percentage				82.446

The main contributor to the safety factor value in our study is the friction component of the equation (Fig. 6). In similar case study [32], the aftermath of the slope stability simulation is to establish a threshold slope angle above which sliding is likely to occur. In our case study, a threshold of 33.2 degrees for a mean safety factor lesser than 1.5 was established. The results of the FOSM model applied in our case show that the uncertainty about safety factor decreases as increases the slope angle. Hence the safety factors in regions with steep slope are more reliable than those obtained in regions with gentle slopes.

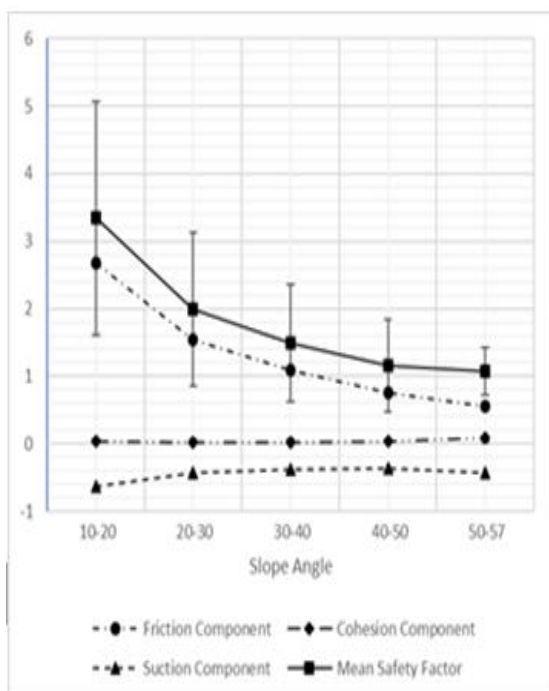


Figure 5. Components contribution to safety factor values for different range of slope angle and standard deviation about the safety factor values for each range of slope angle.

The AUC value of the FOSM model applied is 0.810. The ROC curve of the landslide susceptibility model is shown in Fig. 7. Comparison of landslide susceptibility models

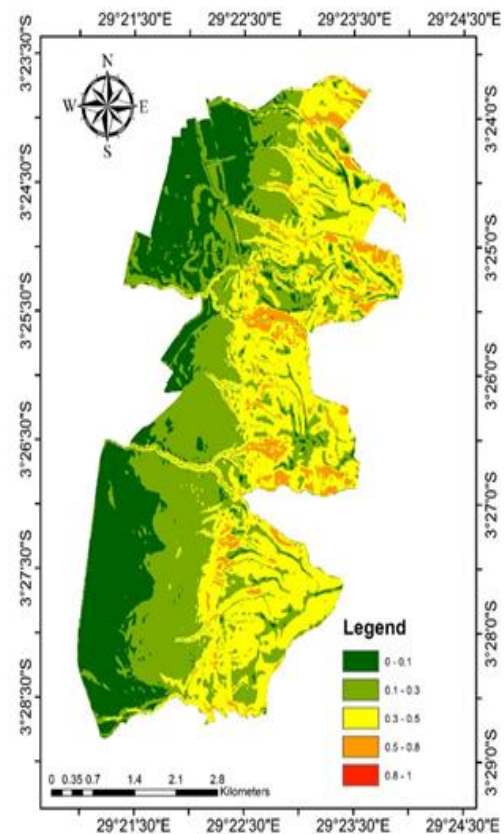


Figure 6. Landslide susceptibility map (FOSM<1.5)

Comparatively the susceptibility maps produced with LR and FOSM models differs. Cohen's kappa coefficient is only 0.199 meaning the spatial correlation is at most fair. However, the good accuracy capacity of both models was corroborated by the AUC (Fig. 7). The spatial extent of each susceptibility level, the corresponding percentage of correct predictions are summarized in Table 5. The spatial comparison of the two susceptibility maps is shown in Fig. 8. Zero shows spatial concordance between landslide susceptibility levels. Negative values show that landslide susceptibility levels obtained with FOSM are lower compared with the susceptibility levels obtained with LR. The difference increasing from -1 to -4. Positive values show the contrary. The ideal spatial concordance between susceptibility levels for the two maps occurs in 41.1% of the study area. The opposite happens in 9.9% of the study area (Table 6). The 0 and +1 concordance happens in 81.8%. This means that spatial ideal concordance and spatial level difference where LR level is one level lower than the FOSM level occupy 81.1% of the study area. This confirms the ability of the physical model to more

accurately differentiate the susceptibility levels in the intermediary levels (69.545% of the study area for FOSM with 72.12% of correct predictions) than the statistical model which is more accurate in the extreme susceptibility levels (35.441% of the study area for LR with 30.271% of correct predictions).

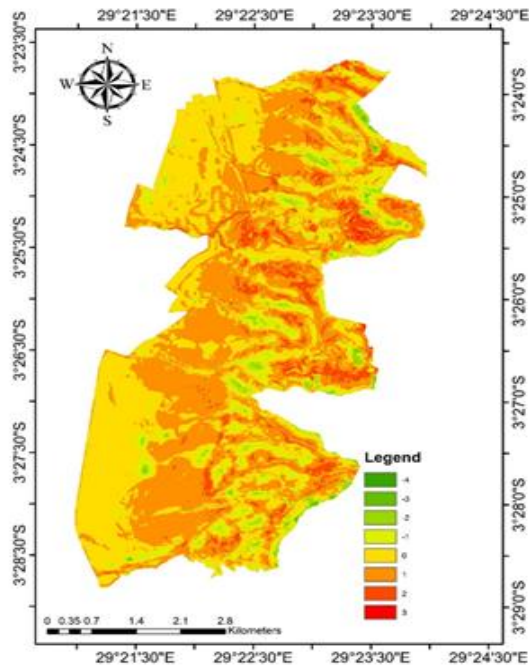


Figure 7. Spatial agreement map between LR and FOSM maps.

Table 5. Spatial extent of the levels defined by LR and FOSM susceptibility map

Susceptibility Level	LR Model		FOSM Model	
	Study area %	Training group %	Study area %	Training group %
Very High	1.898	1.668	0.003	0.022
High	8.480	6.035	5.414	2.894
Moderate	11.429	7.549	33.048	28.652
Low	24.012	22.722	36.406	43.468
Very Low	54.181	62.026	25.128	24.964

Table 6. Cross comparison of levels difference

	FOSM Map					Total
	Very Low	Low	Moderate	High	Very High	
Very Low	22.7	26.2	5.2	0.1	0	54.2
Low	2.1	7.8	13.1	0.9	0	24
Moderate	0.2	1.5	8.3	1.4	0	11.4
High	0.1	0.7	5.3	2.3	0	8.5
Very High	0	0.1	1.1	0.7	0	1.9
Total	25.1	36.4	33	5.4	0	100

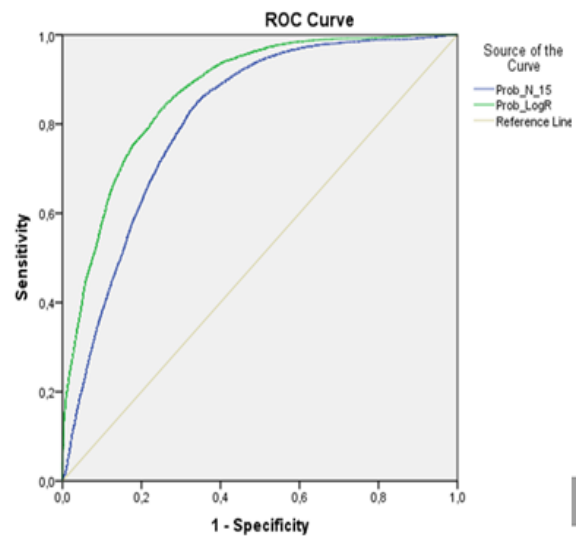


Figure 8. ROC curves of landslides susceptibility models

V. CONCLUSION

Landslide susceptibility assessment using statistical or deterministic models are widely used. However, they represent different approaches. While deterministic models use mechanical and hydrological properties, the statistical models use regression and weights potential triggering factors. In this study, landslide susceptibility using logistic regression and First order second moment method models was mapped. Further, the results obtained are compared with a landslide inventory map we built using literature and imagery. The AUC curve results obtained showed an independently good accuracy for both models. The Kappa statistics showed a fair correlation at most. Spatial comparison of the results shows a better accuracy for FOSM in intermediate levels and for LR in extreme levels. Landslide susceptibility assessment showed both model could be applied with satisfactory results. However, a combination of the two models should be explored.

REFERENCES

- [1]. UNOSAT/UNOSAT, "Landslide in Rutunga, Bujumbura Rural Province, Burundi (as of 17 Apr 2015) - Burundi | ReliefWeb," 2015. [Online]. Available: <https://reliefweb.int/map/burundi/landslide-rutunga-bujumbura-rural-province-burundi-17-apr-2015>. [Accessed: 02-Mar-2018].
- [2]. RTNB Burundi, "Les contreforts des Mirwa nécessitent une protection particulière RTNB Burundi," 19/03/2018, 2018. [Online]. Available: <http://www.rtnb.bi/fr/art.php?idapi=2/2/147>. [Accessed: 04-Jun-2018].

- [3]. L. Nibigira, S. Draïdia, and H.-B. Havenith, "GIS-Based Landslide Susceptibility Mapping in the Great Lakes Region of Africa, Case Study of Bujumbura Burundi," in *Engineering Geology for Society and Territory - Volume 2*, Cham: Springer International Publishing, 2015, pp. 985–988.
- [4]. D. Kubwimana, L. Ait Brahim, M. Bousta, O. Dewitte, A. Abdelouafi, and T. Bahaj, "Landslides susceptibility assessment using AHP method in Kanyosha watershed (Bujumbura-Burundi): Urbanisation and management impacts," *MATEC Web Conf.*, vol. 149, p. 02071, 2018.
- [5]. L. Montrasio and R. Valentino, "A model for triggering mechanisms of shallow landslides," *Nat. Hazards Earth Syst. Sci.*, vol. 8, no. 5, pp. 1149–1159, 2008.
- [6]. R. L. Baum, W. Z. Savage, and J. W. Godt, "TRIGRS—A Fortran Program for Transient Rainfall Infiltration and Grid-Based Regional Slope-Stability Analysis, Version 2.0." Denver Publishing Service Center, Denver, p. 75, 2008.
- [7]. R. T. Pack, D. G. Tarboton, and C. N. Goodwin, "SINMAP - A stability index approach to terrain stability hazard mapping," *Manuel*, pp. 1–75, 2003.
- [8]. M. Anderson, D. Lloyd, and M. Kemp, "Hydrological design manual for slope stability in the Tropics," *Overseas Road Note 14*, 1997.
- [9]. D. R. Montgomery and W. E. Dietrich, "A physically based model for the topographic control on shallow landsliding," *Water Resour. Res.*, vol. 30, no. 4, pp. 1153–1171, Apr. 1994.
- [10]. Z. Wu et al., "A comparative study on the landslide susceptibility mapping using logistic regression and statistical index models," *Arab. J. Geosci.*, vol. 10, no. 8, 2017.
- [11]. D. Tien Bui, Q. P. Nguyen, N. D. Hoang, and H. Klempe, "A novel fuzzy K-nearest neighbor inference model with differential evolution for spatial prediction of rainfall-induced shallow landslides in a tropical hilly area using GIS," *Landslides*, pp. 1–17, 21-Apr-2016.
- [12]. H. Bourenane, M. S. Guettouche, Bouhadad, and Braham, "Landslide hazard mapping in the Constantine city, Northeast Algeria using frequency ratio, weighting factor, logistic regression, weights of evidence, and analytical hierarchy process methods," *Arab. J. Geosci.*, vol. 9, no. 2, pp. 1–24, Feb. 2016.
- [13]. D. Tien Bui, T. A. Tuan, H. Klempe, B. Pradhan, and I. Revhaug, "Spatial prediction models for shallow landslide hazards: a comparative assessment of the efficacy of support vector machines, artificial neural networks, kernel logistic regression, and logistic model tree," *Landslides*, vol. 13, no. January, pp. 361–378, Apr. 2015.
- [14]. C. Conoscenti, M. Ciaccio, N. A. Caraballo-Arias, Á. Gómez-Gutiérrez, E. Rotigliano, and V. Agnesi, "Assessment of susceptibility to earth-flow landslide using logistic regression and multivariate adaptive regression splines: A case of the Belice River basin (western Sicily, Italy)," *Geomorphology*, vol. 242, pp. 49–64, Aug. 2015.
- [15]. S. C. Oliveira, J. L. Zêzere, S. Lajas, and R. Melo, "Combination of empirically-based and physically-based methods to assess shallow slides susceptibility at the basin scale," *Nat. Hazards Earth Syst. Sci. Discuss.*, vol. 2016, no. December, pp. 1–37, 2016.
- [16]. F. Cervi, M. Berti, L. Borgatti, F. Ronchetti, F. Manenti, and A. Corsini, "Comparing predictive capability of statistical and deterministic methods for landslide susceptibility mapping: a case study in the northern Apennines (Reggio Emilia Province, Italy)," *Landslides*, vol. 7, no. 4, pp. 433–444, Dec. 2010.
- [17]. N. Lu and J. Godt, "Infinite slope stability under steady unsaturated seepage conditions," *Water Resour. Res.*, vol. 44, no. 11, p. n/a-n/a, Nov. 2008.
- [18]. Direction Générale de l'Environnement, "Communication nationale sur les changements climatiques," 2005.
- [19]. D. J. Varnes, "Slope Movement Types and Processes," *Transp. Res. Board Spec. Rep.*, no. 176, pp. 11–33, 1978.
- [20]. L. Ayalew and H. Yamagishi, "The application of GIS-based logistic regression for landslide susceptibility mapping in the Kakuda-Yahiko Mountains, Central Japan," *Geomorphology*, vol. 65, no. 1–2, pp. 15–31, Feb. 2005.
- [21]. L. J. Wang, M. Guo, K. Sawada, J. Lin, and J. Zhang, "A comparative study of landslide susceptibility maps using logistic regression, frequency ratio, decision tree, weights of evidence and artificial neural network," *Geosci. J.*, vol. 20, no. 1, pp. 117–136, Feb. 2016.
- [22]. S. Park, C. Choi, B. Kim, and J. Kim, "Landslide susceptibility mapping using frequency ratio, analytic hierarchy process, logistic regression, and artificial neural network methods at the Inje area, Korea," *Environ. Earth Sci.*, vol. 68, no. 5, pp. 1443–1464, Mar. 2013.

- [23]. I. Yilmaz, "Comparison of landslide susceptibility mapping methodologies for Koyulhisar, Turkey: conditional probability, logistic regression, artificial neural networks, and support vector machine," *Environ. Earth Sci.*, vol. 61, no. 4, pp. 821–836, Aug. 2009.
- [24]. Y. Wu et al., "Landslide susceptibility assessment using frequency ratio, statistical index and certainty factor models for the Gangu County, China," *Arab. J. Geosci.*, vol. 9, no. 2, p. 84, Feb. 2016.
- [25]. H. R. Pourghasemi, "Analysis and evaluation of landslide susceptibility: a review on articles published during 2005 – 2016 (periods of 2005 – 2012 and 2013 – 2016)," vol. 2016, 2018.
- [26]. C. Meisina and S. Scarabelli, "A comparative analysis of terrain stability models for predicting shallow landslides in colluvial soils," *Geomorphology*, vol. 87, no. 3, pp. 207–223, 2007.
- [27]. S. Beguería, "Changes in land cover and shallow landslide activity: A case study in the Spanish Pyrenees," *Geomorphology*, vol. 74, no. 1–4, pp. 196–206, 2006.
- [28]. J. Choi, H. J. Oh, H. J. Lee, C. Lee, and S. Lee, "Combining landslide susceptibility maps obtained from frequency ratio, logistic regression, and artificial neural network models using ASTER images and GIS," *Eng. Geol.*, vol. 124, no. 1, pp. 12–23, Jan. 2012.
- [29]. D. Zizioli, C. Meisina, R. Valentino, and L. Montrasio, "Comparison between different approaches to modeling shallow landslide susceptibility: A case history in Oltrepo Pavese, Northern Italy," *Nat. Hazards Earth Syst. Sci.*, vol. 13, no. 3, pp. 559–573, 2013.
- [30]. T. L. Tsai, P. Y. Tsai, and P. J. Yang, "Probabilistic modeling of rainfall-induced shallow landslide using a point-estimate method," *Environ. Earth Sci.*, vol. 73, no. 8, pp. 4109–4117, 2015.
- [31]. E. Arnone, Y. G. Dyalynas, L. V. Noto, and R. L. Bras, "Parameter Uncertainty in Shallow Rainfall-triggered Landslide Modeling at Basin Scale: A Probabilistic Approach," *Procedia Earth Planet. Sci.*, vol. 9, pp. 101–111, 2014.
- [32]. W. C. Haneberg, "A Rational Probabilistic Method for Spatially Distributed Landslide Hazard Assessment," *Environ. Eng. Geosci.*, vol. 10, no. 1, pp. 27–43, 2004.
- [33]. G. Zhou, T. Esaki, Y. Mitani, M. Xie, and J. Mori, "Spatial probabilistic modeling of slope failure using an integrated GIS Monte Carlo simulation approach," *Eng. Geol.*, vol. 68, no. 3–4, pp. 373–386, 2003.
- [34]. I. ASTM, "Standard Test Method for Direct Shear Test of Soils Under Consolidated Drained Conditions. ASTM D3080 - 11," 2011.
- [35]. G. M. Saulnier, K. Beven, and C. Obled, "Including spatially variable effective soil depths in TOPMODEL," *J. Hydrol.*, vol. 202, no. 1–4, pp. 158–172, 1997.
- [36]. V. Bagarello, M. Iovino, and D. Elrick, "A Simplified Falling-Head Technique for Rapid Determination of Field-Saturated Hydraulic Conductivity," *Soil Sci. Soc. Am. J.*, vol. 68, no. 1, p. 66, 2004.
- [37]. S. Zacharias and G. Wessolek, "Excluding Organic Matter Content from Pedotransfer Predictors of Soil Water Retention," *Soil Sci. Soc. Am. J.*, vol. 71, no. 1, p. 43, 2007.
- [38]. ASTM, "Standard Test Method for Particle-Size Analysis of Soils D422-63," ASTM Stand. Test Method, vol. D422–63 (R, no. Reapproved 2007, pp. 1–8, 2007.
- [39]. ASTM, "Standard Test Methods for Laboratory Determination of Density (Unit Weight) of Soil Specimens D7263-09," ASTM Int., vol. D7263-09, pp. 1–7, 2009.
- [40]. D. Sawatzky, G. Raines, and G. Bonham-carter, "Spatial Data Modeller," pp. 1–19, 2010.

Gervais Shirambere "Comparative assessment of landslide susceptibility by logistic regression and first order second moment method: Case study of Bujumbura Peri-Urban Area, Burundi. "International Journal of Engineering Research and Applications (IJERA) , vol. 8, no.8, 2018, pp 28-37